Trans. JSASS Aerospace Tech. Japan
Vol. 14, No. ists30, pp. Pf_131-Pf_140, 2016

Demonstration of Innovative System Design for Twin Micro-Satellite: Hodoyoshi-3 and -4

By Yoshihiro TSURUDA,[1)] Yoshihide AOYANAGI,[1)] Toshiki TANAKA,[1)] Takeshi MATSUMOTO,[1)] Shinichi NAKASUKA,[1)] Seiko SHIRASAKA,[2)] Masayasu MATSUI[3)] and Ichiro MASE[3)]

[1)]*Department of Aeronautics and Astronautics, The University of Tokyo, Tokyo, Japan*
[2)]*Keio University, Kanagawa, Japan*
[3)]*The Next Generation Space system Technology Research Association, Kanagawa, Japan*

(Received July 31st, 2015)

Between June 2011 and March 2014, The University of Tokyo, in collaboration with The Next Generation Space system Technology Research Association, developed a twin micro-satellite: Hodoyoshi-3 and -4 to demonstrate and establish an innovative system design and a cost-effective development process for the mass production of micro-satellites in the future based on a new concept called "Hodoyoshi", which means "reasonably reliable". On June 19, 2014, the two satellites were successfully launched into Sun Synchronous Orbit, at an altitude of approximately 630 km. To date, we met several objectives with regard to system performance on-orbit, a considerable amount of mission data including Earth observation images. This project demonstrates system architecture design methods, integration and test processes, and on-orbit operation methods such as recovery functions from anomalies. The project is currently undergoing evaluation, under which the results of the operation are being reviewed with regard to the Hodoyoshi concept. This paper explains the Hodoyoshi concept, providing examples of hardware and software design, and arriving at a reasonable interface design and coordination. The paper also introduces the major characteristics of the satellites, and explains the key features and approaches of microsatellite development to realize cost-effectiveness.

Key Words: Cost-Effective, Reasonably Reliable, Reusability, System Design, Hodoyoshi

1. Introduction

Since the launch of the first CubeSat in 2003, the number of microsatellites (class of satellites that weigh less than 100 kg) launched has increased steadily. Applications of microsatellites have also expanded beyond technology demonstration and educational purposes at universities. Furthermore, the number of commercial missions (e.g., Earth observation) has gradually increased with the expansion and improvement of capabilities of microsatellites. In this regard, The University of Tokyo, in collaboration with The Next Generation Space system Technology Research Association (NESTRA), has developed a 50-kg-class twin microsatellite. Through this project, the two parties aim to demonstrate and establish an innovative system design and a cost-effective development process for the mass production of microsatellites in the future.

This project aims to develop an innovative method of system engineering based on the "Hodoyoshi" concept [1–3], for microsatellite development. Hodoyoshi is a Japanese word that means reasonably reliable. The word can also be interpreted as "more than enough is too much" or "good enough." In the case of a complex system such as a spacecraft, a large number of parameters are associated with the system components and its interfaces. Therefore, typically, the cost of development of such a system increases in proportion to the physical properties of the satellite, such as size and mass, as well as in proportion to its performance and reliability. However, to achieve a successful satellite mission within reasonable cost, it is necessary to find the optimal point between "high-cost, high-performance" and "low-cost, low-performance." The optimal point depends on the characteristics of a system including satellite specifications, and also on the project team, motivation, resources, and objectives. [4] This project focuses on reusability of the design process for microsatellites and their components, based on the concept of Hodoyoshi. Reusability is one of the approaches to reduce the number of elements used to develop a system.

2. Hodoyoshi-3 and -4 System Characteristics

This section introduces the major characteristics of the Hodoyoshi-3 (H3) and -4 (H4) project and the system designs of the two microsatellites.

2.1. Major specifications

Table 1 shows the major characteristics of the flight models of the H3 and H4. The primary mission of the H3 and H4 is Earth observation using various optical sensors. The H3 has two different cameras: –one with low resolution and another with medium resolution. The cameras have a ground sampling distance (GSD) of 250 m and 40 m, respectively. H4, on the other hand, has a relatively high-resolution camera with a GSD of 6–10 m. Furthermore, the microsatellites possess various secondary mission instruments, including wide-angle mini-cameras, hosted payload boxes, a technology demonstration module, and a UHF data receiving system for store-and-forward mission. The inclusion of such instruments enables rapid, on-orbit demonstration of new technology, and low-cost commercial usage such as advertisement in space. The designs of the two satellites are based on standardized system architecture. They carry various advanced on-board equipment, of reasonable cost and reliability. The equipment have been developed using Japanese commercial technology under the Hodoyoshi program. The components mostly consist of commercial off-the-shelf (COTS) devices for the purpose of cost saving.

Table 1. System characteristics of Hodoyoshi-3 and -4.

	Hodoyoshi-3 (H3) (2014-033-F) [40015]	Hodoyoshi-4 (H4) (2014-033-B) [40011]
Size	0.5 × 0.5 × H:0.7 m	0.5 × 0.6 × H:0.8 m
Mass	56 kg (including H_2O_2)	64 kg (including Xe gas)
Orbit	SSO: 612 × 665 km e = 0.0037, i = 97.97deg LTAN 10:30 AM	SSO: 612 × 650 km e = 0.0027, i = 97.97deg LTAN 10:30 AM
Epoch	2014/06/19 15:27:05 (UTC)	2014/06/19 15:27:03 (UTC)
Mission		
Main Imager	Earth Observation using multispectral optical sensors	
	- MCAM (1pc) GSD: 38m (swath: 78km) 3 bands (R, G, NIR) - LCAM (1pc) GSD: 240m 3 bands (R, G, B)	- HCAM (1pc) GSD: 6.3m (swath: 25km) 4 bands (R, G, B + NIR)
Sub Imager	- VGA mini-camera (Wide Angle: 5pcs) (Narrow Angle: 1pc)	- VGA mini-camera (Wide Angle: 6pcs) - Extra-Wide Angle: 1pc
Secondary Payload	Store & Forward Data Collection Platform UHF Signal Receiving System (Receiver + Antenna)	
	Hosted payloads (regulated 10cm cubic box) 3 cubes	4 cubes
	Hetero-constellation experiment	
Propulsion	Monopropellant H2O2	Xe Micro Ion Propulsion
Technical DEMO	✓ New Batteries ✓ New OBC Board ✓ New Micro Camera ✓ Thin Film Solar Cell	✓ New Materials ✓ Thermal Control Device ✓ Satellite Charging Measurement Device
Bus		
Structure	Al-alloy honeycomb panel and isogrid base plate	
Thermal	Multi-Layer Insulator (MLI), Flexible OSR, and paint	
Commun-cation	Telemetry (TLM) / Command (CMD): S-band CCSDS TLM Downlink: 32/64kbps, CMD Uplink: 4kbps	
	Mission data downlink: X-band 10Mbps CCSDS (demonstrated up to 350Mbps on Hodoyoshi-4)	
EPS	Generation: max 130W (GaInP2/GaGa/Ge SolarCell) Consumption: average 40 - 50W, max 70W Battery: 5.8Ah, Nominal 28V (24 – 32V) (Li-Ion Battery)	
AOCS	Sun pointing Mode ⇔ Earth pointing Mode 3-axis stabilization (control accuracy: +/- 0.5deg) by using Reaction Wheels, MTQs, GPS, Star Tracker, Fiber Optical Gyro, Sun Sensors, Magnetometers	
CDH	OBC: Advanced On-board computers (OBCs) for Main Data Handing (MOBC) and Attitude Control (AOBC) powered by SOI-SoC Technology Software: Hodoyoshi-SDK + C2A based Application	

2.2. Configuration design

Figure 1 shows the conceptual image of design transition from a baseline design to those of H3 and H4, based on the launch vehicle (LV) condition. The two microsatellites are designed within the regulated envelop (footprint: 0.5 m × 0.5 m area, height: < 0.8 m) based on the Dnepr LV typical regulation for microsatellite. This envelop condition is larger than the Japanese LV H-IIA piggyback launch (footprint: 0.5 m × 0.5 m area, height: < 0.5 m). Through the interface coordination with the launch service provider of Dnepr LV, the parties understood that, like the mass of a satellite, its footprint also affects its launch cost. For a typical cluster launch, LV companies aim to maximize the number of payloads and therefore, to reduce the launch cost, the footprint should be as small as possible. As shown in Fig. 1, our preliminary design is based on the H-IIA piggyback condition. Therefore, to increase the mission payload capacity, we updated the configuration design to include a basic structure for installing common bus components and an additional mission bay on the roof area of the basic structure. In this project, we used mission bays of two different sizes to match the required mission payload scales. This concept enables satellites to accept various user requirements while maintaining cost-effectiveness.

Figure 2 shows the actual configuration design of H3 and H4 during launch and on-orbit after separation from the LV. In the case of H4, the tip of the imager's hood was slightly higher than desired. However, it was accepted because of its low impact on the footprint under the launch condition. After separation from the LV's upper stage, each satellite deploys a Solar cell Array Paddle (SAP) to guarantee power generation.

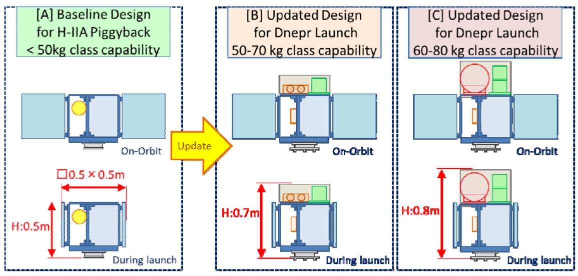

Fig. 1. Configuration concept considered launch vehicle condition.

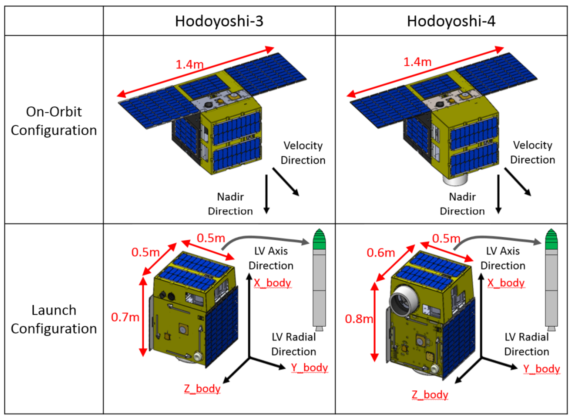

Fig. 2. Designed configuration for H3/H4 during launch and on-orbit.

Figures 3 and 4 compare the characteristics of the Earth pointing surface (called PZ-Surface) and the SAP surface (called MZ-Surface) of H3 and H4. A remarkable difference is observed between H3 and H4, with regard to the layout of equipment on the PZ-Surface. Major mission instruments, including the aperture of the observation camera and antenna, are located on the PZ-Surface. Therefore, this surface is usually kept facing the nadir direction during observation missions such as image shooting and antenna pointing for high-rate telecommunication using X-band downlink. This mode is called the "Earth pointing mode." On the other hand, the MZ-Surface is usually kept facing the sun, because the largest number of solar cells (140) are located on this surface after SAP deployment.

Figure 4 shows the real features of the SAP surface. This surface is similar for both the H3 and H4. As shown in the figure, the density of the solar cell mounted on the SAP is maximized as much as possible for effective power generation. During house-keeping operations such as battery charging, the MZ-Surface is kept facing the sun to generate enough power. This mode is called "sun pointing mode". [5]

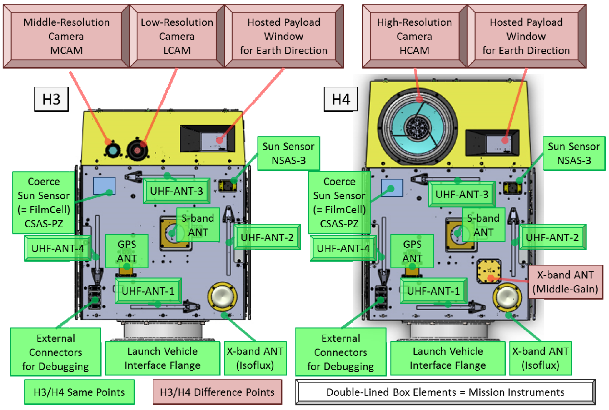

Fig. 3. Characteristics of H3/H4 earth-pointing surface (PZ).

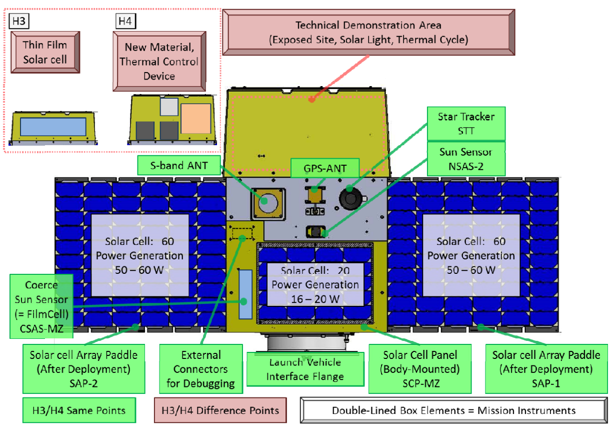

Fig. 4. Characteristics of H3/H4 solar cell array paddle surface (MZ).

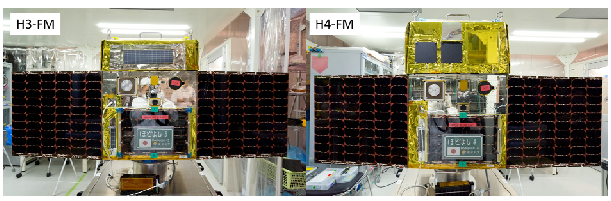

Fig. 5. Real features of H3/H4 FM solar cell array paddle surface.

As explained above, the sun pointing mode and Earth pointing mode are the two major satellite modes, which are realized by three-axis control using reaction wheels (RWs). Corresponding to the accuracy of control, each mode has a coarse state and a fine state.

To achieve three-axis stabilization at the initial operation phase, the satellite attitude is controlled by magnetic torquers (MTQs). The following two modes help control satellite attitudes in various situations:

✓ B-dot mode for reducing tumbling rate
✓ Spin-Sun pointing mode for controlling spin rate around Z-axis of satellite and pointing the spin axis to the sun

Because the power consumption of MTQs is lower than that of RWs, these modes can be executed under the tumbling condition. Therefore, these modes using MTQs are also used for recovery from attitude anomaly. Fundamentally, the mode transition is executed by CMD uplink.

3. Key Concepts for Realizing Reasonable System

This section introduces the key concepts of system design, based on the Hodoyoshi concept, to realize a reasonable and cost-effective system. It is important to maintain a balance between the expected results and costs associated with time, budget, and resources. The Hodoyoshi concept is especially suitable for projects under relatively limited conditions such as university or small-scale projects. The concept fundamentally accepts "re-try" and considers it a primary principle. A space mission is a situation that requires "one-time action", which means that any mistakes are strictly unacceptable. If there are too many one-time actions in a single satellite mission, it might increase costs as many on-ground tests may be required to be conducted before the launch. Therefore, we aim to reduce the number of one-time actions by combining the re-try functions (as active action) with a supportive configuration hardware design (as passive effect). The following sections show four examples of our approach.

3.1. Solar cell area coverage maximization

Solar cell area coverage is one of the most important factors for satellite survivability. In case of large satellites, solar cells usually tend to be located on only one surface such as a large SAP surface. This configuration is adopted because of an extremely robust attitude control system. On the other hand, in the case of typical university satellites such as the CubeSat, body-mounted solar cells are frequently used because of their limited capability.

In this regard, we considered an effective solar cell layout to ensure sufficient power generation in all modes of satellite operation, without depending on the robustness of the attitude control system. One of the key points of consideration was to maintain a balance between primary power generation by the SAP surface and secondary power generation by body-mounted solar cells. It is not effective to allocate more solar cells than necessary. Therefore, we designed body-mounted solar cells for H4, as shown in Fig. 7. This configuration is common to both H3 and H4. As shown in Fig.7, body-mounted solar cell panels are located on four surfaces—PX, MX, PY, and MY—excluding the PZ-Surface. In the case of H3 and H4, we did not place any solar cells on the PZ-Surface because of reasons such as the lack of enough area and requirement of a stable antenna pattern that combines the UHF, S-band, and X-band.

To mitigate the risk of the state of deadlock by attitude anomaly, solar cells are laid out on five surfaces of six cubic structures. The redundant generation of power by body-mounted solar cell panels helps realize the re-try operation in the case of attitude anomaly. Considering these features, we formulated the operation strategy of the satellites before launch, and incorporated the strategy into the real operations of H3 and H4.

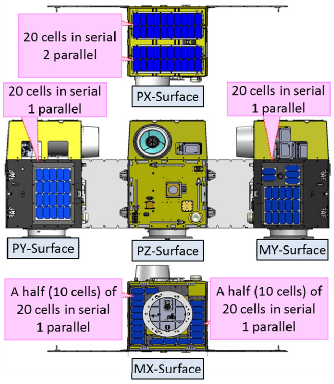

Fig. 6. An example of H4 body-mounted solar cell panel layout.

Figure 7 shows examples of developed body-mounted solar cell panels for each of the five surfaces. The shapes of these panels were defined based on the equipment layout of each surface. To achieve effective integration, we did not use glue to directly mount the solar cells on the surfaces of the structures, and rather used glue to first mount the solar cells on 3 mm thin carbon fiber reinforced plastic (CFRP) substrate panels and then attached the panel subassemblies to the surfaces of the structures using bolts. Based on the results of thermal analysis, a multi-layer insulation (MLI) was inserted between the structure panel and solar cell panel subassembly to keep the inside temperature stable, in case of H3 and H4.

This is an example of effective interface design with regard to mechanical integration and thermal control design. [6)]

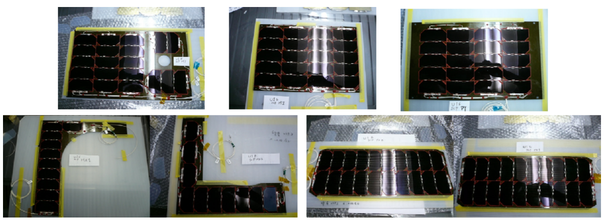

Fig. 7. Real features of body-mounted solar cell panel.

3.2. Implementation of reset function

To avoid hang-up state of a digital device in a satellite, implementing reset function is very important. Generally, a device such as an OBC is operated through an internal software. It is extremely difficult to develop software with no bugs; a software should be considered to have potential anomalies like an endless loop. Therefore, the reset function is regarded as an absolute method of recovery to the initial state. Considering these factors, along with risks associated with software and the implementation of reset function, we defined the priority level for system reset, and organized the flow of signal input for reset and recovery actions.

Figure 8 shows the conceptual diagram of the flow of the reset function designed for the H3 and H4. The concept defines four key components: OBC, S-band Transmitter and Receiver (STRX), Watch Dog timer Box (WDB), and Power Control Unit (PCU). The OBC was developed by an experienced team, and it was based on Silicon on Insulator-System on Chip (SOI-SoC) technology, which enabled the component to tolerate higher radiation. In the case of H3 and H4, we defined two OBCs: MOBC to handle main data and AOBC to control attitude. The functions of both these OBCs can be performed by a single OBC; however, we defined two separate OBCs for effective development, including effective parallel coding and testing, which takes into consideration the requirements of the interface and team members. With regard to allocated functions and interfaces, AOBC is regarded as a slave computer of MOBC. For generalized discussion, we have expressed MOBC as “OBC” in this and the following sections.

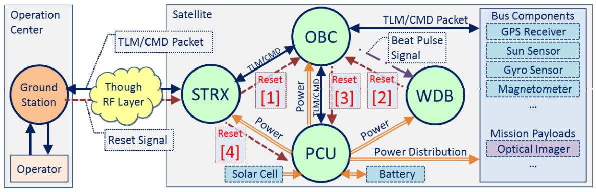

Fig. 8. Conceptual diagram of reset function flow.

An on-ground operator can send reset signal [1] through a CMD uplink to help an OBC to recover from an unexpected hang-up. In case of H3 and H4, the decision to send signals through a CMD uplink is made by an operator after receiving status information, including housekeeping (HK) data, through a TLM downlink.

The typical method of embedded computers, called watch-dog-timer, defines reset signal [2]. For this function, we designed a simple standalone hardware in the case of H3 and H4. Under nominal conditions, the OBC keeps sending the beat pulse signal to the WDB. In case the beat pulse signal stops because of a hang-up, the WDB sends a reset signal to OBC power interface to execute a power reset. The reset signal [2] is regarded as the redundant root of the reset signal [1] supported by a different type of trigger from WDB.

Reset signal [3] is used for the digital controller located on the control board in the PCU. The reset signal [4] is a redundant root for the PCU. In case of H3 and H4, the PCU was developed in accordance with the requirements of the mission plan (how to use) and development plan (how to make, based on the “Hodoyoshi” concept) of the microsatellites. In this context, we regarded the PCU as the lowest priority component among the four key components of the reset function for the microsatellites. Fundamentally, the PCU was designed to perform major functions such as battery charging control and over-current protection through analog circuits. The advanced and autonomous functions of the digital controller in the PCU are performed by the CMD from the OBC.

To realize the reset concept, the robustness of the STRX and WDB must be higher than that of the OBC and PCU. In this regard, we selected an existing STRX component that was demonstrated on a similar orbit in a past microsatellite mission. The circuit design of the WDB is very simple, and therefore, we had sufficient time for its evaluation. In fact, the harness connection of reset signal [4] was removed in the case of H3 and H4 FM because of the lack of enough time for evaluation. The reset signals [1], [2], and [3] are used for on-ground system tests on ground and for actual, on-orbit operations.

3.3. Under voltage control for battery management

To keep a battery under safe state, it is important to consider suitable actions based on parameters such as state of charging (SOC) or depth of discharge (DOD) that denote the battery's capacity. The battery protections are categorized into two major actions: over-level action and under-level action, as per current (I), voltage (V), and temperature (T). In general, the capacity of a battery (SOC or DOD) is expressed as a function of three variables: I, V, and T.

$SOC = f(I, V, T)$

To reduce complexity, we simplified this model based on the properties of the battery cell selected by us and the experimental data on ground; the above relation can be expressed as:

$SOC = f_1(V)\ [I_1 \text{ to } I_2, T_1 \text{ to } T_2],\ f_2(V)\ [I_2 \text{ to } I_3, T_2 \text{ to } T_3], \ldots$

(where f (V) consists of a combination of linear proportions of battery voltage within a specific voltage range.)

By using this concept, we established a reasonable, cost-effective method of battery management. The dead state of a battery, which means break down of charge/discharge function, must be avoided to be able to realize the reasonable strategy, including the "re-try" operation. This section focuses on the under voltage control (UVC) function.

Table 2. An example of UVC actions and level setting.

UVC Level	Action (examples based on operation experience)
S/W UVC Lv.1 (26.8 – 28.0V)	power budget safer state by turning off the mission instruments' power port
S/W UVC Lv.2 (26.5 – 27.5V)	Transit to the low-power mode without depending attitude. (No-Attitude control, core-function only)
S/W UVC Lv.3 (25.0 – 26.5V)	Reduce the power consumption in low-power by minimizing S-Tx RF power mode and Battery heater setting. minimum power mode

Table 2 shows an example of the UVC function and level setting designed for the on-orbit operation of H3 or H4. Three levels of UVC have been defined for stepwise execution of suitable actions. The voltage range seen in the table is an example based on the battery voltage curve. During actual operation, the value for each level is registered as a voltage threshold parameter in software, and it can be changed using the uplink parameter. The OBC monitors the voltage measured by PCU, and compares it to the registered threshold in the basic cycle. If the measured value falls below the threshold, the OBC executes defined actions at each level. The UVC is supported by the OBC software. The defined actions includes power saving by turning off the mission instruments and transition to low-power consumption mode such as the Standby Mode or the Safe Mode in H3/H4 system without depending on attitude.

3.4. Reconfigurable OBC software architecture

Important functions of the OBC software are introduced in this section. It is highly difficult to change or modify the configuration of the software after launch of the satellite due to time constraints. Typically, the software of the satellite OBC includes re-programming function and/or parameter tuning for duty ratio of housekeeping actions, variables for on-board estimation, attitude control gain, and so on. Sufficient variation tests must be conducted to enable re-programming of complete or partial source code during actual operation, prior to uplink of the updated source file. The values can be changed in the case of parameter tuning, however, new actions are not added in case of on board sequence. The "Command Centric Architecture (C2A)" method is taken into consideration to facilitate effective operation. [7)]

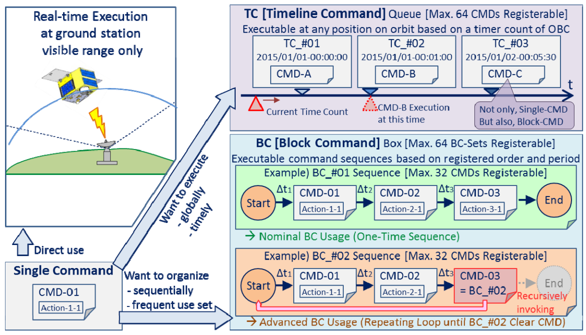

Fig. 9. Conceptual diagram of command functions design.

Figure 9 illustrates an example of conceptual diagram of the command functions design of H3/H4. Fundamentally, a single CMD is sent within the visible range of the ground station for real-time operation. However, considering the context of our operation plan and cost-effective implementation, we came up with the following requirements: timely CMD execution globally including out of range of the ground station (e.g., taking images of polar region), and sequentially organizing sets of CMDs frequently used (e.g., attitude maneuvering).

In this context, we defined a concept of timeline command (TC) and block command (BC) as shown in Fig.9. Complete or partial re-programming functions and variable parameters through uplink have also been installed within the on-board software of H3/H4. In addition to the traditional functions, application tools supported by the TC and BC functions have been applied to enable advanced and flexible operation strategy. The operation tasks can be executed in time at the desirable positions on the orbit through introduction of new CMDs to the TL queue. On the other hand, a new sequence of function can be generated post launch using the BC function. The BC function has two major advantages, namely, reduction of the number of CMD sent and generation of on-board autonomous events and long-term cyclic events. The order, interval, and contents of CMD can be recognized through CMD uplink in the BC function.

4. Development Process

This section describes the combined development process of the H3 and H4 with actual performed order. The development flow of initiation of the Engineering Model (EM) to completion of the Flight Model (FM) is illustrated in Fig. 10.

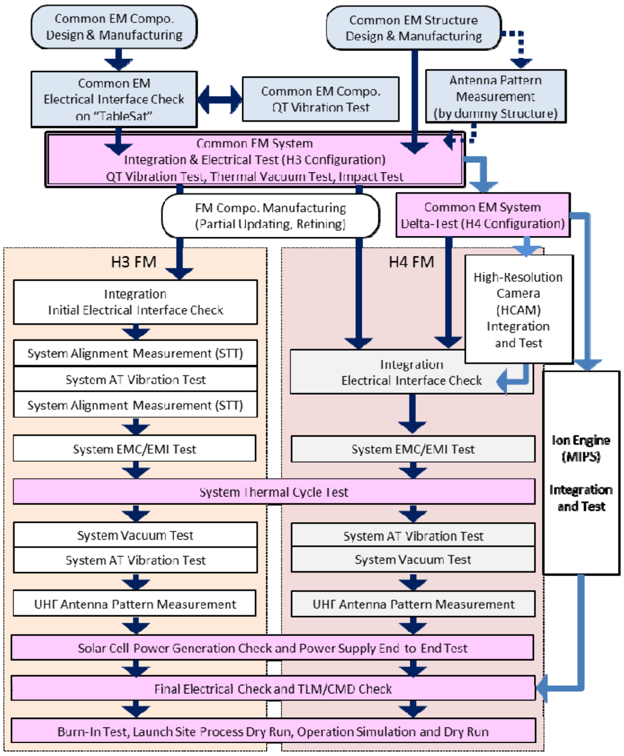

Fig. 10. Development Flow of H3/H4 combined process.

4.1. Electrical tests on table

Prior to integration of the system including the structural and mechanical elements, a testbed was established on table (called as the "TableSat" in this project). The main objectives of TableSat test are as follows:

- ✓ To check the power distribution interface between the electrical power subsystem (EPS) components and other components. The EPS components consist of a PCU and two types of Power Distribution Unit (PDU), namely the Bus-component Power Distribution Unit (BPDU) and the Mission-instrument Power Distribution Unit (MPDU) in case of H3/H4.
- ✓ To check the electrical signal interface between the OBC and other components such as RS422, TTL, LVTTL, Analog +/-5V, etc.
- ✓ To validate the fundamental framework of the software and interface drivers.

The TableSat is useful in electrical interface tests as it is easier to change the configuration of the test by inserting break out box (BOB) between the harness connections. The BOB helps to measure electrical properties such as current, voltage, frequency, and pulse pattern of the signal-line and the power-line, respectively.

4.2. EM integration and electrical check

A common EM system has been established to create provision for two FMs for effective development. The system has been designed on the basis of similarities and differences in the characteristics of the H3 and H4. Fundamental configuration is targeted in case of H3, whereas delta-test configuration is used for H4 to replace some components or instruments such as HCAM and MIPS.

Figure 11 and 12 show actual testing and checking of the EM. The process of integration, electrical checks, and fundamental functional tests were conducted in a hand-made clean room at The University of Tokyo. test cables and facilities were prepared in-house by the project team to reduce expenditure. Qualification Test (QT) level environmental tests were conducted at the Nano-satellite Test Center, Kyushu Institute of Technology (KIT), Kita-Kyushu.

The electrical and the environmental tests, using common EM, enabled validation of system design as well as identification of refining points for designing of the FM component.

Fig. 11. Common EM Integration and Electrical Check at The University of Tokyo, Clean Room (2012/09/01-2013/03/31).

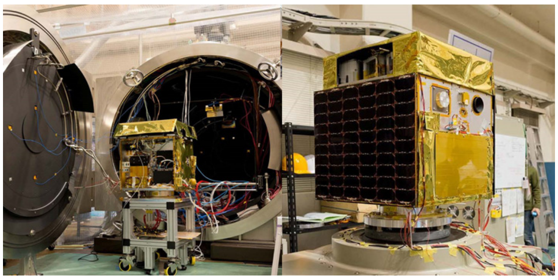

Fig. 12. Common EM Thermal Vacuum Test and QT Vibration Test at Nano-satellite Test Center, KIT (2012/11/10-2012/011/28).

4.3. FM integration and electrical check

FM integration was initiated in the beginning of October 2014 with H3 integration. It was followed by H4 integration at the end of November 2014. Figures 13 to 17 represent the actual set up for FM checks and tests. The satellites were arranged in parallel fashion in a clean room as illustrated in Fig. 13. The FM implementation activities were conducted in a sequence. However, several AT tests were conducted simultaneously to save time through effective team organization. This process of combined development for two similar systems is one of the achievements of the H3/H4 project. All FM checks and tests were finished by the end of March 2014.

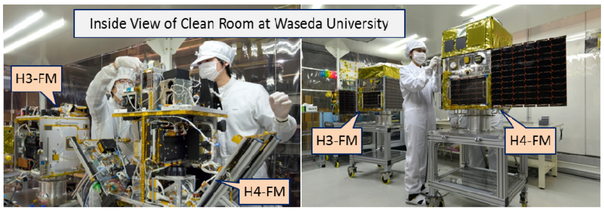

Fig. 13. H3/H4 FM Integration and Electrical Checkout at Waseda University, Clean Room (2013/10/01-2014/03/31) [performed one by one in order (Mechanical Process and electrical interface check), in parallel (TLM/CMD tests)].

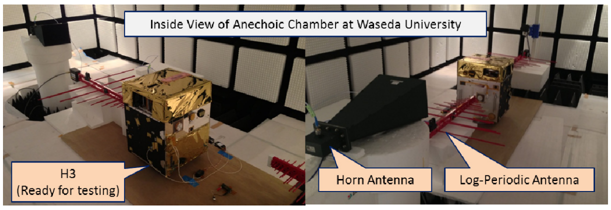

Fig. 14. H3/H4 FM EMC/EMI Test at Waseda University, Anechoic Chamber (2014/01/14-2014/01/16) [performed one by one in order].

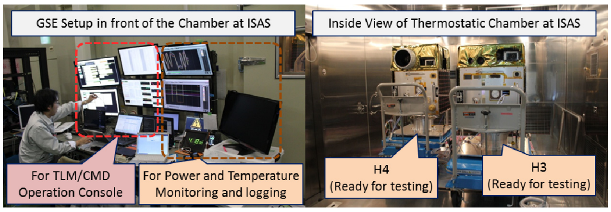

Fig. 15. H3/H4 FM Thermal Cycle Test Pictures at ISAS, Thermostatic Chamber (2015/01/27-2014/01/31) [performed simultaneously].

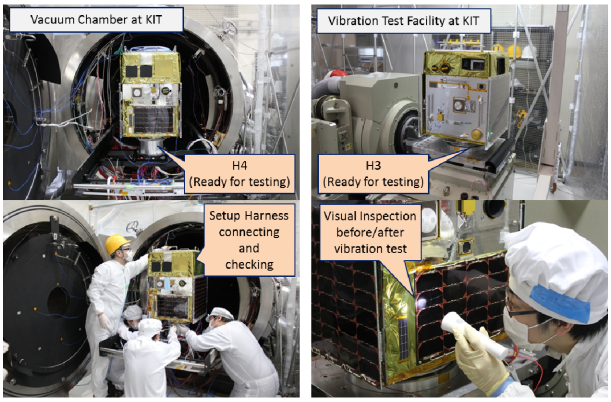

Fig. 16. H3/H4 FM Vacuum Test and AT Vibration Test at Nano-satellite Test Center, KIT (2014/02/03-2014/02/21) [performed one by one in parallel operation].

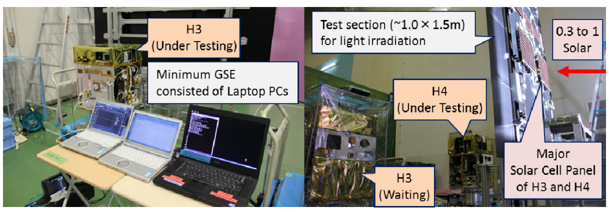

Fig. 17. H3/H4 FM Solar Cell Power Generation Check, Power Supply End-to-End Test at ISAS (2014/02/24-2014/02/28) [performed one by one in order].

4.4. FM EMC/EMI Tests

The FM Electromagnetic Compatibility (EMC) and Electro-Magnetic Interference (EMI) tests were conducted to study the tolerance of RF receiving systems of satellites towards RF emission from launch vehicle. The satellite system functions were validated using digital and analog on-board circuits during S-band or X-band downlink. In these tests, several RF signal bands such as UHF, L-band, S-band, and X-band are measured using log-periodic antenna and horn antenna to cover multi-band RF signals in the anechoic chamber as illustrated in Fig. 14.

4.5. FM thermal cycle test

The FM thermal cycle test was performed to obtain validation against thermal condition using thermostatic chamber at the Institute of Space and Astronautical Science (ISAS), Sagamihara. The chamber was large enough to simultaneously accommodate two satellites easily as illustrated in Fig. 15 in order to perform the test. Two sets of ground support equipment (GSE) were arranged in front of the chamber to minimize the length of the test harness. These sets include the equipment allocated at the ground station for actual operation. The nominal temperature for this test ranged between 0°C to +40°C taking the range of operational temperature of the battery into consideration. The test functioned in four cycles. The constant temperature state was continued for over 12 hours in the third cycle for the highest and the lowest cases, respectively. This enabled to study the impact of long-term exposure of high or low temperature on the performance of the satellite. The function test and simulation of actual operation were carried out during the third cycle using TLM or CMD console and GSEs.

4.6. FM vacuum test and AT vibration test

The FM vacuum test and the AT vibration test were performed using a vacuum chamber and a vibration stage at KIT as illustrated in Fig. 16. For effective implementation, the project team was divided into two sub teams namely the vacuum test team and the vibration test team. Under the vibration test, three types of tests were performed, namely the sign, sign-burst, and random tests for each of 3-axis under the condition of Acceptance Test (AT) level. We performed visual inspection before and after each vibration test. The vacuum test was conducted to rectify the workmanship error in the system, and to study the function under the vacuum condition (in 10^{-4} Pa, after continues 48 hours). The same configuration of TLM/CMD console and GSE was used for this test as in case of the thermal cycle test.

4.7. FM solar cell tests

The FM solar cell power generation check and the power supply end-to-end test were conducted using a large-area pulse solar simulator at ISAS as illustrated in Fig. 17. The two main objectives of these tests are to measure the electrical properties (I-V curve and P-V curve) of each solar cell panel, and to confirm the fitness of the connections passing through PCU from the solar cell power line to the battery power line. The test section of this facility used for this test is large enough to accommodate several solar cell panels.

5. Launch Site Operation

This section briefly introduces the summary of launch site operation. The detailed information is presented by the paper; "As shown in 8), Cluster Launch of Hodoyoshi-3 and -4 Satellites from Yasny by Dnepr Launch Vehicle (ISTS 2015-f-33)."

The launch campaign began on May 22, 2014 and ended on June 7, 2014. During this period, activities like battery installation, charging and final checking of battery, H_2O_2 fueling of the H3 system, activation of xenon tank for the H4 system, and final electrical tests for H3 and H4 were conducted by the project team. After completion of all the checks and tests, the two satellites were integrated on the dispenser of the Dnepr LV upper stage as shown in Fig. 18.

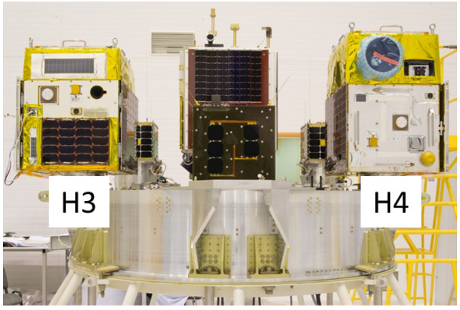

Fig. 18. The final condition of H3/H4 FM integrated on the dispenser of the Dnepr LV upper stage at Yasny Launch Base, in Russia (2014/06/07).

6. Operation Result on Orbit

This section introduces the operation results of the entire satellite system, achievements of major missions, and the lessons learned on the orbit.

6.1. Initial operation results

On June 19, 2014, H3 and H4 were successfully launched into the Sun-synchronous Orbit at an altitude of about 630 km through Dnepr launch vehicle in Russia. Figure 19 illustrates the ground station operation center at The University of Tokyo. As seen in the picture, we arranged monitors of TLM/CMD console to conduct an effective operation. An operator can conduct operation for a single satellite in the case of nominal operation phase. Table 3 illustrates the results of major events of initial operation of H3/H4 on the orbit. The H4 downlinked the first light image taken by a small wide-angled camera after 55 h from launch. It not only included stop-motion pictures but video as well.

Fig. 19. The first AOS operation at the ground station operation center of The Univ. of Tokyo (2014/06/20 08:20-08:49(JST)).

Table 3. Major events of initial operation on orbit of H3/H4.

Date (yyyy/mm/dd)	Major Events
2014/03/31	Completion of Nominal Test schedule for Hodoyoshi-3 and -4 Flight Model
2014/05/22	Start of launch site activities at Yasny in Russia
2014/06/11	End of launch site activities at Yasny in Russia
2014/06/19	Launch as payloads of Dnepr Cluster Launch (2014/06/19 19:11:10 UTC)
2014/06/20	1st – 4th Pass: Initial Signal Acquisition, Solar Paddle Deploy, Spin-Sun Pointing
2014/06/22	First Light of wide-angle small camera image and movie
2014/07/02	Three-axis Sun Pointing achieving
2014/07/04	Three-axis Earth Pointing achieving
2014/07/05	First Light of Low- and Mid-Resolution Camera Image
2014/08/01	First Light of High-Resolution Camera Image

Figure 20 illustrates the sample images taken by the sub imagers of the H3 and H4. These sub imagers provided VGA RGB images in JPEG format with 1–4 fps (frame per second). Thus, we can view the earth in form of a video by combining multiple images taken from the same viewpoint by the satellites at an altitude of 630 km in SSO. This function is not only useful for typical observation, but also to facilitate space utilization in the form of space advertisement. As seen on the right hand side of the image in Fig. 18, we can monitor the complete or partial satellite in form of "self-shooting" images for housekeeping actions or to check the condition of deployable elements on the basis of the direction of the aperture of the camera.

These cameras were developed by Tokyo University of Science and were integrated into the mission model by the team from The University of Tokyo. The head module of the camera is light-weight with dimensions of 30 mm × 30 mm × 20 mm. Thus, we can install them on any redundant area of the satellite structure.

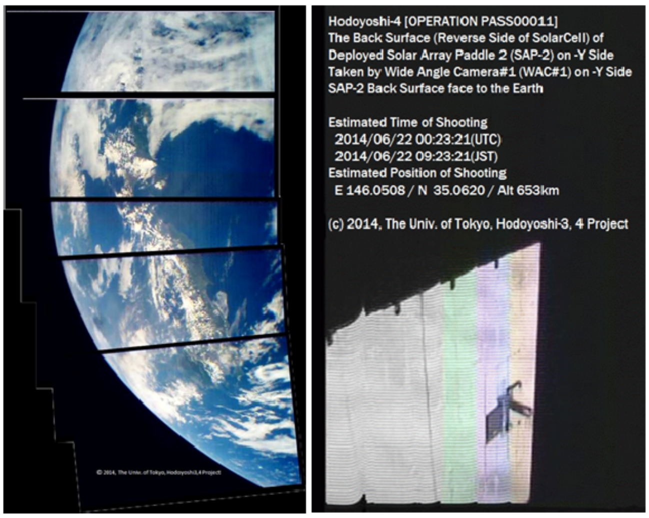

Fig. 20. Sample images of the sub imagers of H3/H4 (VGA wide-angle mini-camera). The left shows continues images by H3 taking broad area centered around Japan (2014/06/20). The right shows the self-shooting Image of the deployed SAP of H4 (2014/06/22).

6.2. Results of the main mission (optical observation)

This section introduces the optical observation results of the MCAM/LCAM of H3 and the HCAM of H4. Sample images captured by MCAM/LCAM of H3 in a single shot can be seen in Fig. 21. Figure 22 illustrates the sample images after combining nine contiguous images captured by the MCAM. The LCAM is able to capture a larger area such as the East-Japan region whereas the MCAM is able to capture a focused area such as the urban region of Tokyo. Both the cameras comprise an area-sensor which enables them to shoot images without depending on attitude disturbance.

The cameras were developed by Tokyo University of Science and The University of Tokyo. The lens, imager IC, and the data handling unit of MCAM/LCAM mainly comprise the COTS device. These cameras have a general Red-Green-Blue (RGB) Bayer type image sensor. In the case of MCAM, a multi-band pass filter is mounted in front of the aperture of the imager to enable 3-band (G: 550–580 nm, R: 650–690 nm, NIR: 890–930 nm) spectroscopic imaging, whereas in LCAM, an IR cut filter is mounted. Data processing of MCAM and LCAM is carried out by an FPGA board (OS: LINUX, image processing: OpenGL) [9–11]. Both the MCAM and LCAM of H3 are capable of capturing an enlarged image of a specific region of the target. This can be useful in disaster and environmental monitoring of abroad to middle ranged area.

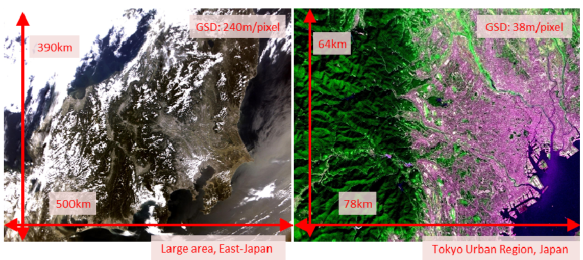

Fig. 21. Examples of H3-LCAM/MCAM images (one-shot image) (Left: East Japan, 2014/08/10, RGB true-color process, Right: Tokyo urban region, 2014/10/17, Natural color expression; R/G/B by converted from R/IR/G).

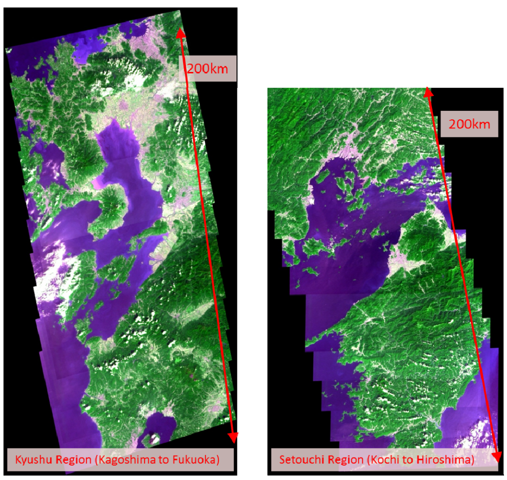

Fig. 22. H3-MCAM sample images combined continuous nine images (Left: Kyushu region, Japan, 2014/10/24, Right: Setouchi region, Japan, 2014/10/19) [Natural color expression; R/G/B by converted from R/IR/G].

Figure 23 shows the sample images captured by the HCAM of H4. The HCAM was developed by The University of Tokyo and NESTRA in collaboration with experienced companies. The optical system of HCAM comprises a Ritchey–Chretien type reflecting telescope whose aperture diameter is 150 mm and focal length is 1000 mm. The primary mirror of the HCAM is made of ceramic glass and the lens barrel is made of CFRP. Both of these materials are relatively light-weight and robust for dynamic changes in thermal condition.

The HCAM consists of a push-broom scan type multi-spectrum sensor with four bands, namely, R, G, B, and NIR. The imager has two identical NIR line sensors, which are capable of setting their gain parameters individually, and thus enable expansion of the dynamic range.[11] Space Wire between the HCAM and the Science data Handling Unit (SHU) provides the interface for communication.

The sample picture seen in Fig. 23 shows the mount region, coast region, agricultural area, and residential area of Katsuura-city, Chiba-prefecture, Japan. The focused image shows the performance of identifying a road between rice fields whose width is less than 10 m. Thus, the resolution of the HCAM images can be categorized as advanced class among similar past microsatellites.

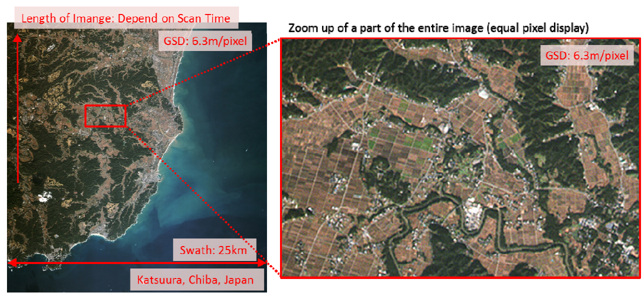

Fig. 23. An example of H4-HCAM image (Katsuura, Chiba, Japan, 2014/12/24, RGB true-color process).

6.3. Results of the secondary mission

This section briefly introduces the additional unique achievements of H3 and H4. In addition to the main optical observation mission, H3 and H4 also comprises different secondary mission instruments as shown in Table 1 in the previous section. The secondary mission instruments include the data collection platform experiment for “Store & Forward” service in the future using UHF signal receiving system, [12] expansion of new space utilizing opportunity enabled by hosted payloads with 10 cm regulated cubic box, [13] demonstration of new propulsion system such as the monopropellant H_2O_2 injection system [14] for H3, Xe micro ion propulsion system [15–16] for H4, and new technology demonstration (high-speed X-band downlink, [17] new batteries, [18–19] OBC board, [20] micro camera, [20] thin film solar cell, functional materials, thermal control device, and satellite charging measurement device). The achievements of the secondary mission instruments can be applied to next generation space system including micro-satellites.

7. Conclusion

For innovative space utilization, we have been developing a 50-kg-class twin-satellite called “Hodoyoshi-3 (H3) and Hodoyoshi-4 (H4)” since June 2011. On June 19, 2014, both H3 and H4 were successfully launched into the sun-synchronous orbit at an altitude of approximately 630 km through the Dnepr launch vehicle in Russia.

In this paper, we have described an innovative design of the system based on the Hodoyoshi concept from the viewpoint of system design, ground testing, and orbit operation. We have also introduced the important characteristics of the satellites and explained the key features and approaches of microsatellite development to enable cost-effective process and orbit operation.

We hope that this achievement can create opportunities for further discussion on methodologies for innovative system design for mass-production of micro-satellites in the future.

Acknowledgments

This research was supported by a grant from the Japan Society for the Promotion of Science (JSPS) through the “Funding Program for World-Leading Innovative R&D on Science and Technology (FIRST Program),” initiated by the Council for Science and Technology Policy (CSTP). The authors also acknowledge the constant support and dedication of the Hodoyoshi-3 and -4 project team and supporters.

References

1) Nakasuka, S.,: From Education to Practical Use of Nano-satellites – Japanese University Challenge towards Low Cost Space Utilization -, 8th IAA Symposium on Small Satellite for Earth Observation, Berlin, April, 2011
2) Tsuruda Y., Nakasuka, S., Matsui M. and Mase I.: Reasonably Reliable System Design and Operation for Twin Satellite: Hodoyoshi-3 & 4, 1K09, 58th Space Sciences and Technology Conference, Nagasaki, Japan, November, 2014 (in Japanese).
3) Mase I., Matsui M., Tsuruda Y. and Nakasuka S.: Initial performance in orbit of Hodoyoshi-3 and Hodoyoshi-4, 1K10, 58th Space Sciences and Technology Conference, Nagasaki, Japan, November, 2014 (in Japanese).
4) Shirasaka, S., Tsuruda, Y., Nakasuka, S., Matsui, M. and Mase, I.: Implementation and Evaluation of Reasonably Reliable Systems Engineering for Micro-Satellites through Hodoyoshi-3 and -4 Projects, Paper presented at the 30th International Symposium on Space Technology and Science, 2015-t-07, Kobe, Japan, 5-10 July 2015.
5) Miyata, K. and Nakasuka, S.: On-Orbit Evaluations of the Three Axis Stabilization Performances of Standard Micro-Satellite Buses, Paper presented at the 30th International Symposium on Space Technology and Science, 2015-f-88p, Kobe, Japan, 5-10 July 2015.
6) Ito, M., Mase, I., and Yamaguchi, K.: Thermal Control System and Performance on Orbit of Three Microsatellite using Common Bus System, 1K18, 58th Space Sciences and Technology Conference, Nagasaki, Japan, November, 2014 (in Japanese).
7) Takisawa, J., Kobayashi, S., Huong, T., Kimura, S. and Nakasuka, S.: Micro/Nano-satellites On-board Software Framework Design and Its Implementation in Hodoyoshi Satellites, 5th Nano-satellite Symposium, NSS-05-0101, Tokyo, Japan, 20-23 November 2013.
8) Yoshimoto, S., Nakasuka, S., Tsuruda, Y., Aoyanagi, Y., Tanaka, T., Sahara, H., Ohira, T., Araki, Y., Mase, I., Ito, M., Kainov, V., Karandaev and A., Silkin, O.: Cluster Launch of Hodoyoshi-3 and -4 Satellites from Yasny by Dnepr Launch Vehicle, Paper presented at the 30th International Symposium on Space Technology and Science, 2015-f-33, Kobe, Japan, 5-10 July 2015.
9) Aoyanagi Y., Iwasaki Y., Nakasuka S., Ebinuma T., Kimura S. and Narumi T.: Initial result of Hodoyoshi-3, 4 earth observation mission, 58th Space Sciences and Technology Conference, Nagasaki, Japan, November, 2014 (in Japanese).
10) Narumi, T., Aoyanagi, Y. and Kimura, S.: Low-Cost Intelligent Parallel Image Acquisition System for Small Satellite, Paper presented at the 30th International Symposium on Space Technology and Science, 2015-f-90p, Kobe, Japan, 5-10 July 2015.
11) Aoyanagi, Y., Iwasaki, A., Nakasuka. S., Ebinuma, T., Kimura, S. and Narumi, T.: Result of Hodoyoshi-3 and -4 Earth Observation Missions, Paper presented at the 30th International Symposium on Space Technology and Science, 2015-n-06, Kobe, Japan, 5-10 July 2015.
12) Matsumoto, T., Matsui, M., Nakasuka, S., Yamaguchi, K., Shibayama, Y. and Fukami, T.: Development of Store and Forward System on Micro-Satellite : Hodoyoshi3&4, Paper presented at the 30th International Symposium on Space Technology and Science, 2015-f-93p, Kobe, Japan, 5-10 July 2015.
13) Tanaka, T., Satogata, R., Shibayama, Y., Yamaguchi, K., Hamaguchi, R., Nakazawa, K. and Nakasuka, S.: Utilization of HODOYOSHI-3&4 Hosted Payloads in the Field of Advertisement and Entertainment, Paper presented at the 30th International Symposium on Space Technology and Science, 2015-f-23, Kobe, Japan, 5-10 July 2015.
14) Sakuma, T., Sahara, H., Miyashita, N., Kuramoto, Y., Matsui, M., Yoshimoto, S., Tsuruda, Y. and Nakasuka, S.: Development and On-Orbit Demonstration of the Propulsion System Based on 60wt% Hydrogen Peroxide for Microsatellites, Paper presented at the 30th International Symposium on Space Technology and Science, 2015-f-40, Kobe, Japan, 5-10 July 2015.
15) Koizumi, H., Komurasaki, K., Aoyama, J. and Yamaguchi, K.: Engineering Model of the Miniature Ion Propulsion System for the Nano-satellite, Trans. JSASS Space Tech. Japan, **12**(2014), pp.Tb_19-Tb_24.
16) Koizumi, H. and Nakasuka, S.: Miniature Ion Thruster Propulsion System, In-Flight Operation First operation of an ion thruster on a small satellite (less than 100 kg), press release by School of Engineering, The Univeristy of Tokyo, 12 December 2014. http://www.t.u-tokyo.ac.jp/etpage/release/2014/141212-01.html
17) Fukami, T., Watanabe, H., Saito, H., Tomiki, A., Mizuno, T., Iwakiri, N., Shigeta, O., Nunomura, H., Kojima, K., Shinke, T. and Kawamoto, K.: Field Tests of 348 Mbps High Speed Downlink System for 50-kg Class Satellite, Paper presented at the 30th International Symposium on Space Technology and Science, 2015-f-89p, Kobe, Japan, 5-10 July 2015.
18) Tanaka, K., Tsuruda, Y., Sone, Y., Ishikawa, M., Yamagata, M., Kono, M., Kimura, S., Nakazawa, K., Maeda, K., Hayakawa, Y., Shirasaka, S., Nakasuka, S., Fukuda, S., Saito, H.: In-orbit demonstration of the energy storage devices using demonstration module of HODOYOSHI, 2K06, 58th Space Sciences and Technology Conference, Nagasaki, Japan, November, 2014 (in Japanese).
19) Yamagata, M. and Ishikawa, M.: The first lithium-ion battery with ionic liquid electrolyte demonstrated in Space, Press release by Kansai University, 16 December 2014 (in Japanese). http://www.kansai-u.ac.jp/global/guide/pressrelease/2014/No32.pdf
20) Kimura, S., Narumi, T., Tanaka, K., Tsuruda, Y. and Nakasuka, S.: High-Performance on-board computer for micro- and nano-satellites and its on-board demonstration, 1K17, 58th Space Sciences and Technology Conference, Nagasaki, Japan, November, 2014 (in Japanese).